



# High-mobility polymer space-charge-limited transistor with grid-induced crystallinity

Yu-Chiang Chao<sup>a</sup>, Mu-Chun Niu<sup>a</sup>, Hsiao-Wen Zan<sup>b,\*</sup>, Hsin-Fei Meng<sup>a,\*</sup>, Ming-Che Ku<sup>b</sup>

<sup>a</sup> Institute of Physics, National Chiao Tung University, 1001 Ta Hsueh Rd., 300 HsinChu, Taiwan

<sup>b</sup> Department of Photonics and Institute of Electro-Optics, National Chiao Tung University, 1001 Ta Hsueh Rd., 300 HsinChu, Taiwan

## ARTICLE INFO

### Article history:

Received 28 June 2010

Received in revised form 8 September 2010

Accepted 12 September 2010

Available online 26 October 2010

### Keywords:

Vertical transistor

Space-charge-limited current

## ABSTRACT

The vertical mobility of a polymer film prepared on a textured substrate is enhanced from  $10^{-5}$  cm<sup>2</sup>/Vs to  $10^{-3}$  cm<sup>2</sup>/Vs by a slow drying process which is unattainable in planar substrate. Highly ordered structure is observed for polymer film treated with high-boiling-point solvent and slow solvent annealing. The enhanced vertical mobility enables the polymer space-charge-limited transistor (SCLT) capable of outputting current density as high as 100 mA/cm<sup>2</sup> while maintaining good current gain and on-off ratio. Such vertical transistor is able to drive high-power devices or mechanical actuator in large-area and flexible array.

© 2010 Elsevier B.V. All rights reserved.

## 1. Introduction

Flexible electronics based on solution-processed semiconductors is an exciting emerging technology with the potential applications with very large areas. It enables displays and sensor arrays to cover the surfaces of clothes, buildings, robots, and cars [1,2]. In such large-area array, the pixel size may be over one centimeter and transistors need to drive high-power devices in the pixel as an organic light-emitting diode with high luminance or a motor and other mechanical actuator in robotic applications. For current output over 100 mA it is difficult to achieve using polymer field-effect transistors. Indeed for a channel length of 50 micron typically made by shadow mask the drain current is only 4 mA for channel width as long as 100 cm, given the carrier mobility of 0.1 cm<sup>2</sup>/Vs, drain bias of 20 V, and capacitance of 10 nF/cm<sup>2</sup>. In principle, the 100 cm channel width can be made by 50 pairs of 1 cm long inter-digitated source and drain fingers, resulting in a 1 cm by 1 cm active area. Nevertheless in addition to the insufficient current output, the fabrication of this structure

is fragile because any defect would break the entire finger. Furthermore, the operation voltage of organic field-effect transistor is usually over 20 V, so the Joule heating and power consumption will be a major problem for high-current applications. Polymer field-effect transistor is therefore not suitable for the driving of high-current load in the large-area flexible arrays.

Organic vertical transistors offer another approach to this requirement [3–10]. It has intrinsically low operation voltage and the current is directly proportional to its surface area for easy scaling up. One of the most successful vertical transistors is the space-charge-limited transistor (SCLT) which is a solid-state version of vacuum tube triode, with a metal grid embedded in an organic diode to control its vertical current [7–10]. SCLT shows low-operation voltage, below 1 V, and has a robust fabrication using self-assembled sub-micron plastic spheres as the shadow mask [9]. However, so far its current density ( $J_c$ ) is only 1 mA/cm<sup>2</sup> due to the poor vertical mobility of the polymer. While the field-effect mobility of P3HT and some other polymers is over 0.1 cm<sup>2</sup>/Vs, the vertical bulk mobility is only  $10^{-5}$  cm<sup>2</sup>/Vs. The surface treatment for the gate dielectric enhances the chain alignment near the interface but not in the bulk. Besides, the high carrier density at the interface also increases the mobility by filling the traps.

\* Corresponding authors. Tel.: +886 35731955.

E-mail addresses: [hsiaowen@mail.nctu.edu.tw](mailto:hsiaowen@mail.nctu.edu.tw) (H.-W. Zan), [meng@mail.nctu.edu.tw](mailto:meng@mail.nctu.edu.tw) (H.-F. Meng).

In this work we demonstrate that the polymer vertical mobility can be greatly enhanced by a slow drying process using high-boiling-point solvent, i.e. solvent annealing, in a textured surface with 200 nm scale defined by the grid. The vertical columns promote the chain alignment of P3HT during the slow solvent annealing and result in an ordered structure unattainable in planar substrate. The vertical mobility is raised from  $4 \times 10^{-5} \text{ cm}^2/\text{Vs}$  to  $2 \times$

$10^{-3} \text{ cm}^2/\text{Vs}$  and the SCLT can deliver output current density as high as  $100 \text{ mA}/\text{cm}^2$  while maintaining good current gain and on-off ratio. With such high current density, 100 mA current out-put can be delivered by a  $1 \text{ cm}^2$  active area which is very easy to fabricate with high reliability. With this grid-induced crystallinity SCLT solves the problem of power transistor for large-area flexible electronics.

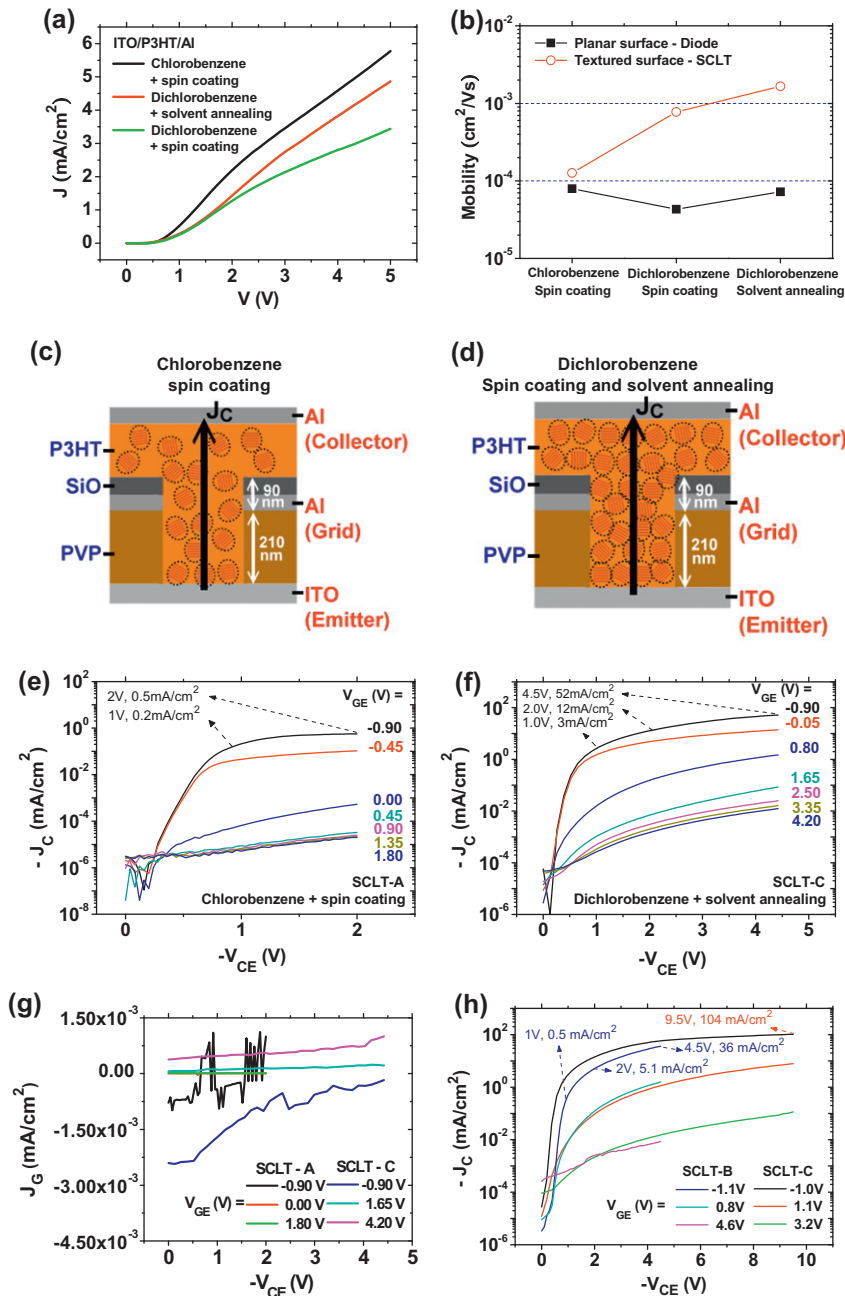


**Fig. 1.** Device characteristics fabricated by various solutions and processes. (a) Diode characteristics. (b) Mobilities of diodes and SCLTs. (c) and (d) Device structure of SCLT. (e) Transistor characteristics of SCLT-A fabricated by chlorobenzene spin coating. (f) Transistor characteristics of SCLT-C fabricated by dichlorobenzene solvent annealing. (g) Grid current density of SCLT-A and SCLT-C. (h) Transistor characteristics of SCLT-B fabricated by dichlorobenzene spin coating and Transistor characteristics of SCLT-C under high collector bias.

## 2. Experimental

The SCLT is fabricated on an ITO glass substrate. Cross-linkable poly(4-vinyl phenol) (PVP) of 210 nm is spin coated and cross-linked on the ITO substrate. Poly (melamine-co-formaldehyde) methylated is utilized as a cross-linking agent for PVP. After treating the PVP surface with 50 W O<sub>2</sub> plasma, the substrate is then submerged into 200 nm positively charged polystyrene spheres (Merck, K6-020) dilute ethanol solution with 0.8 wt.% for 3 min. The substrate is transferred into a beaker with boiling isopropanol solution for 10 s, and then blown dry immediately. Forty nanometer Al and 50 nm SiO are sequentially evaporated as metal base electrode and upper insulating layer. After removing the polystyrene spheres by an adhesive tape (Scotch, 3 M), the PVP at sites without base electrode coverage is removed by 13 min 150 W O<sub>2</sub> plasma treatment. Three hundred and fifty nanometer P3HT is then deposited with or without solvent annealing. For the device prepared by spin coating, P3HT in chlorobenzene or dichlorobenzene is spin coated on the substrate until the film dried. As for the device prepared by dichlorobenzene solvent annealing, P3HT in dichlorobenzene (2.5 wt.%) is spin-coated at 450 rpm for 30 s and then 1200 rpm for 1.2 s to form a P3HT wet film. The wet film is then holding still in the glove box until the film dried. The P3HT film is annealed at 140 °C for 10 min. Finally, the Al collector is deposited to complete the SCLT with active area as 1 mm<sup>2</sup>. Transistor characteristics are recorded using an Agilent E5270B modular parameter analyzer. SEM image is obtained with a field-emission SEM (JEOL JSM-7401). XRD pattern is obtained with high resolution X-ray diffractometer, D1, Bede.

## 3. Results and discussions

Diodes and SCLTs with P3HT thickness of 350 nm are prepared from chlorobenzene (b.p. ~130 °C) and dichlorobenzene (b.p. ~180 °C) to understand the influence of solvent and drying process on the characteristics of devices. Because of the high boiling point of dichlorobenzene, the drying time is 7 s for spin coating P3HT chlorobenzene solution while it is 4 min for spin coating P3HT dichlorobenzene solution. Longer drying time about 20 min is achieved by a solvent annealing procedure which is the first spin coat P3HT dichlorobenzene solution for a short time then letting P3HT dichlorobenzene wet film dry slowly in the glove box. The drying time is visually judged by the change in film color. Diode structure and characteristics are shown in Fig. 1a. The output current density ( $J$ ) of the P3HT diode prepared by spin coating chlorobenzene is higher than the one prepared by spin coating dichlorobenzene. With dichlorobenzene solvent annealing,  $J$  is enhanced but still inferior to the one achieved by chlorobenzene spin coating. The mobility, deduced from  $J$  follows space-charge-limited current (SCLC), of the diode prepared by spin coating P3HT chlorobenzene solution is therefore the highest one among various diodes as shown in Fig. 1b. The influence of the solvent and drying process on the SCLT is, however, not in the

same trend as in diode as shown in Fig. 1e–h. The structure of SCLT is shown in Fig. 1c and d. The active layer of SCLT is fabricated by spin coating P3HT chlorobenzene solution (SCLT-A), spin coating P3HT dichlorobenzene solution (SCLT-B), and spin coating P3HT dichlorobenzene solution for a while then letting wet film dry slowly (SCLT-C). The ITO emitter is commonly grounded and the Al collector is negatively biased at collector-to-emitter voltage ( $V_{CE}$ ).  $J_C$  is obtained by dividing output current by device active area of 1 mm<sup>2</sup>. The grid-to-emitter voltage ( $V_{GE}$ ) is varied to modulate  $J_C$ . As the transistor is turned on with  $V_{GE} = -0.9$  V,  $J_C$  of SCLT-C (shown in Fig. 1f) is higher than the one of the SCLT-A (shown in Fig. 1e) for over one order of magnitude. Besides, as shown in Fig. 1h,  $J_C$  is 36 mA/cm<sup>2</sup> for SCLT-B ( $V_{GE} = -1.1$  V and  $V_{CE} = -4.5$  V) while 52 mA/cm<sup>2</sup> for SCLT-C ( $V_{GE} = -1$  V and  $V_{CE} = -4.5$  V).  $J_C$  of the SCLT fabricated by dichlorobenzene is higher than the one fabricated by chlorobenzene. The SCLT fabricated with dichlorobenzene solvent annealing can output higher current than the one fabricated with spin coating. As a whole, high-boiling-point solvent and long drying time enhance the output current. Furthermore, for SCLT-C,  $J_C$  of 104 mA/cm<sup>2</sup> is achieved when  $V_{CE}$  is  $-9.5$  V as shown in Fig. 1h. With operation voltage below 10 V, this transistor is able to delivered 100 mA output current by a 1 cm<sup>2</sup> area which could drive

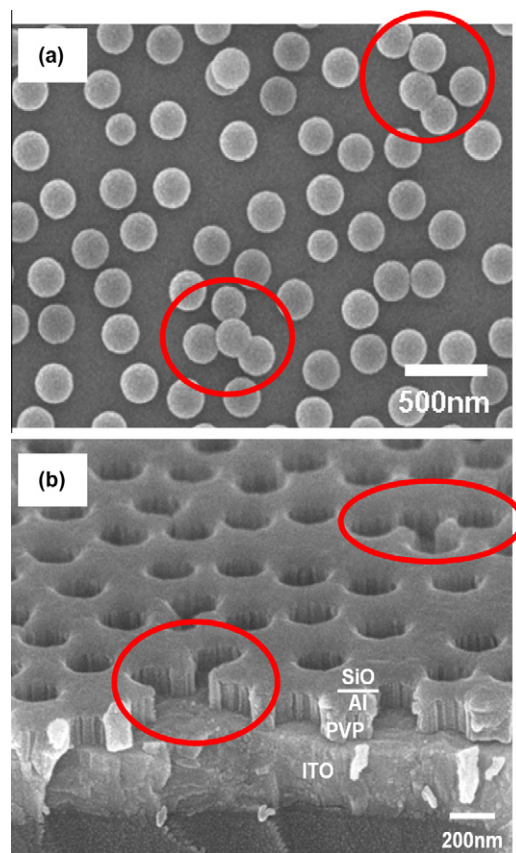


**Fig. 2.** Scanning electron microscopic images. (a) Top view of polystyrene spheres on poly(4-vinyl phenol). (b) The openings form at sites without Al grid.

high-current load in the large-area flexible arrays. As the SCLT is turned off, the off current of SCLT-C is still higher than SCLT-B and SCLT-A. The output current of SCLT is enhanced no matter in on state or off state. However, on/off ratios of these SCLTs are in the same order of  $10^4$ . As shown in Fig. 1g the grid current density ( $J_G$ ) is in the order of  $10^{-4}$  to  $10^{-3}$  mA/cm<sup>2</sup> and hence the current gain  $|J_c/J_G|$  is as large as  $10^4$  to  $10^5$ .

The reason why on and off current of SCLT-C are higher than other devices can be understood from scanning electron microscopy (SEM) images at difference phase of device fabrication. Top view of polystyrene spheres on poly(4-vinyl phenol) (PVP) is shown in Fig. 2a. The openings form at sites without Al grid is shown in Fig. 2b. Although most polystyrene spheres are separate to each other, aggregates contain more than two spheres can still be observed. Large openings will occur at sites with these randomly occurred aggregates. The grid control of the current is strong near the edge of the grid. The vertical carrier channel in the region far away from the grid can not be effectively modulated by grid. As large openings occur, the grid control on the current far away from the grid is small. Despite the on current is benefit from the slow drying process enhanced carrier mobility, the off current can

not be suppressed by  $V_{GE}$  since the grid control on the current in the region away from the grid is less. The off current of SCLT is higher than  $J_G$ .

The mobilities of SCLTs are shown in Fig. 1b. Since the current channel is formed only at the openings, the device active area is recalculated according to the amount of openings for estimating the current density and the mobility. Mobilities deduced from SCLTs are higher than those from diodes except the one of SCLT-A. The highest mobility attainable in SCLT-C is  $2 \times 10^{-3}$  cm<sup>2</sup>/Vs. With high-boiling-point solvent and solvent annealing process, P3HT can be self-organized into semicrystalline lamellar and yield high carrier mobility [11]. The carrier mobility is different in diode and SCLT which can be explained as vertical channel columns induced chain alignment of P3HT during the slow solvent annealing. To understand the reason why mobility increases in SCLT, atomic force microscopy (AFM) images of P3HT surface on textured surface are shown in Fig. 3a–c. The root mean square roughness of 13.6 nm is achieved for spin-coated film from chlorobenzene solution. The roughness increases to 15.3 nm when high boiling point dichlorobenzene is used. As dichlorobenzene solvent annealing process is used, the roughness is further increased to 22.2 nm. It has been demonstrated that polymer

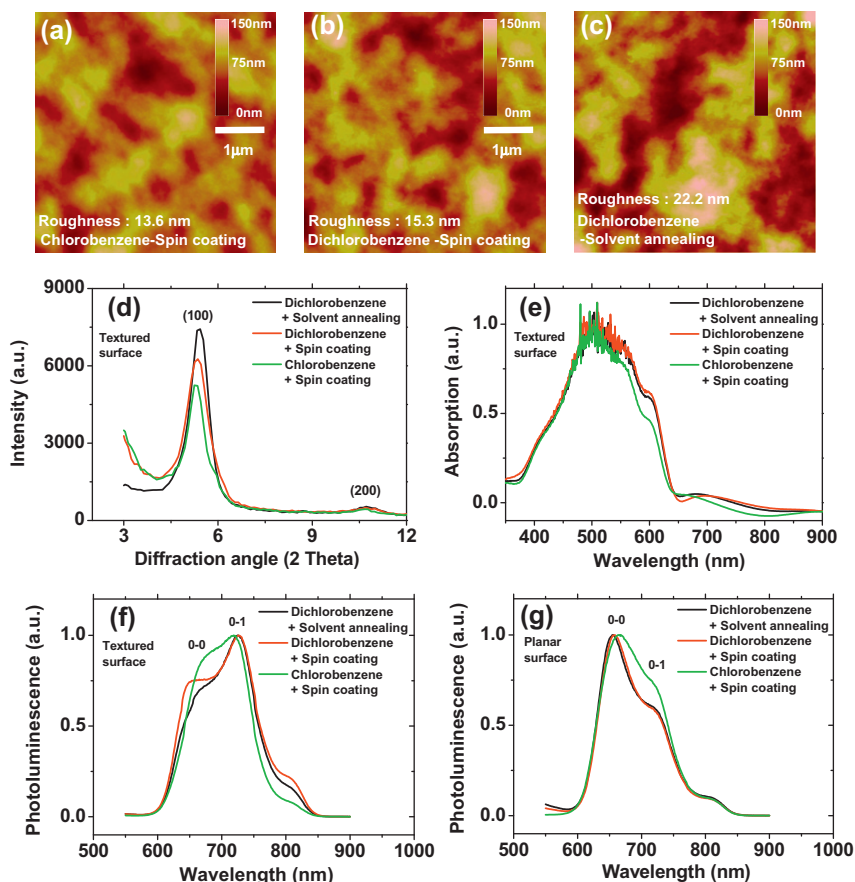


**Fig. 3.** (a–c) Atomic force microscopy images of P3HT surfaces on textured surface. P3HT layers are prepared from three processes those are chlorobenzene spin coating, dichlorobenzene spin coating, and dichlorobenzene solvent annealing. (d) Grazing incidence X-ray diffraction pattern, (e) UV–Vis absorption spectroscopy, and (f) photoluminescence spectroscopy of P3HT film prepared from three processes on textured surface. (g) Photoluminescence spectroscopy of P3HT film prepared from three processes on planar surface.

film with high surface roughness indicates polymer organization [12]. The increased mobility in SCLT may come from the enhanced degree of the polymer chain alignment. To confirm this, grazing incidence X-ray diffraction (GIXRD), UV–visible absorption spectroscopy, and photoluminescence spectroscopy are utilized to get more in-depth information inside the film since AFM images represent only film surface condition. From out-of plane GIXRD spectra shown in Fig. 3d, stronger reflection of the (100) layer can be observed at  $2\theta = 5.4^\circ$  for film prepared with dichlorobenzene solvent annealing [13]. All P3HT films show well-organized intra plane structure which means P3HT self-organizes into two-dimensional  $\pi$ -stacked lamellar structures. The intensity increases when using dichlorobenzene and solvent annealing process. Crystallinity of P3HT is indeed improved by using high boiling point dichlorobenzene and solvent annealing process as illustrated in Fig. 1c and d. Besides, from UV–visible absorption spectra shown in Fig. 3e, prominent vibronic features can be observed at 600 nm for film prepared from dichlorobenzene. Previous work demonstrated that the enhanced vibronic absorption peak indicates strong interchain interactions and enhanced P3HT ordering [14]. This represents the utilization of high boiling point dichlorobenzene helps to induce ordered film with strong inter chain interactions. The influences of  $\pi$ -stacked polymer chains on photoluminescence spectra are shown in Fig. 3f. The 0–0 to 0–1 peak intensity ratio,  $S_R$ , is usually used as an effective probe for disorder [15,16]. The 0–0 peak is forbidden by symmetry in disorder-free aggregates. As disorder occurred the symmetry is broken and the 0–0 emission is allowed. The  $S_R$  is high as P3HT is spin-coated from chlorobenzene; however, as dichlorobenzene is used as the solvent, the  $S_R$  is decreased and reached the lowest value when solvent annealing process is used. This indicates that, on the textured surface, the P3HT film prepared from dichlorobenzene solvent annealing has less disorder while the one prepared from chlorobenzene spin coating has lots of disorder. The mobility is therefore high in P3HT film prepared from dichlorobenzene solvent annealing. Longer drying time may attribute to well-ordered lamellar structure. However, on the planar surface, the film prepared from dichlorobenzene solvent annealing is most disorder while the film prepared from chlorobenzene spin coating is less disorder as shown in Fig. 3g. The difference in photoluminescence spectra of P3HT on textured surface and planar surface reveal the level of disorder and may be used to explain the difference in device performance as shown in Fig. 1. With this grid-induced crystallinity, SCLT treated with dichlorobenzene solvent annealing can output high current which is suitable for large-area flexible electronics. The improved P3HT ordering in grid structure can be explained by improved  $\pi$ - $\pi$  stacking due to nanoconfinement-induced chain alignment. The nanostructure-induced crystallinity in P3HT was also reported by several other groups [17–19]. Coakley et al. reported that P3HT nanopillars with diameters ranged from 20 to 75 nm have

larger hole mobility than P3HT neat film. For pore diameter above 75 nm, the hole mobility falls off and approaches the mobility value for a neat film [17]. In our experiment, with pore diameter as 200 nm, hole mobilities in P3HT nanopillars are still higher than those in neat film. The discrepancy may come from the influences of solvent, drying method, and the pore sidewall properties. The nanostructure-induced crystallinity, however, is a clear phenomenon in all these works.

#### 4. Conclusion

In conclusion, the SCLT capable of outputting current density as high as  $100 \text{ mA/cm}^2$  is realized while maintaining good current gain and on–off ratio. The slow drying process using high-boiling-point solvent is utilized to enhance the polymer vertical mobility. The vertical columns promote the chain alignment of P3HT during the slow solvent annealing and result in an ordered structure unattainable in planar substrate. Such vertical transistor can be used to drive high-power devices or other mechanical actuator in large-area and flexible array.

#### Acknowledgement

This work is supported by the National Science Council of Taiwan under Contract No. NSC98-2628-M-009-001.

#### References

- [1] T. Someya, T. Sekitani, S. Iba, Y. Kato, H. Kawaguchi, T. Sakurai, *Proc. Natl. Acad. Sci. USA* 101 (2004) 9966.
- [2] T. Sekitani, H. Nakajima, H. Maeda, T. Fukushima, T. Aida, K. Hata, T. Someya, *Nat. Mater.* 8 (2009) 494.
- [3] K. Kudo, D.X. Wang, M. Iizuka, S. Kuniyoshi, K. Tanaka, *Thin Solid Films* 331 (1998) 51.
- [4] L.P. Ma, Y. Yang, *Appl. Phys. Lett.* 85 (2004) 5084.
- [5] K. Fujimoto, T. Hiroi, K. Kudo, M. Nakamura, *Adv. Mater.* 19 (2007) 525.
- [6] A.J. Ben-Sasson, E. Avnon, E. Ploshnik, O. Globeman, R. Shenhar, G.L. Frey, N. Tessler, *Appl. Phys. Lett.* 95 (2009) 213301.
- [7] Y.C. Chao, H.F. Meng, S.F. Horng, *Appl. Phys. Lett.* 88 (2006) 223510.
- [8] Y.C. Chao, H.F. Meng, S.F. Horng, C.S. Hsu, *Org. Electron.* 9 (2008) 310.
- [9] Y.C. Chao, Y.C. Lin, M.Z. Dai, H.W. Zan, H.F. Meng, *Appl. Phys. Lett.* 95 (2009) 203305.
- [10] Y.C. Chao, C.Y. Chen, H.W. Zan, H.F. Meng, *J. Phys. D: Appl. Phys.* 43 (2010) 205101.
- [11] G. Li, Y. Yao, H. Yang, V. Shrotriya, G. Yang, Y. Yang, *Adv. Funct. Mater.* 17 (2007) 1636.
- [12] G. Li, V. Shrotriya, J. Huang, Y. Yao, T. Moriarty, K. Emery, Y. Yang, *Nat. Mater.* 4 (2005) 864.
- [13] J.S. Kim, Y. Park, D.Y. Lee, J.H. Lee, J.H. Park, J.K. Kim, K. Cho, *Adv. Funct. Mater.* 20 (2010) 540.
- [14] P.J. Brown, D.S. Thomas, A. Kohler, J.S. Wilson, J.S. Kim, C.M. Ramsdale, H. Sirringhaus, R.H. Friend, *Phys. Rev. B* 67 (2003) 064203.
- [15] J. Clark, C. Silva, R.H. Friend, F.C. Spano, *Phys. Rev. Lett.* 98 (2007) 206406.
- [16] F.C. Spano, J. Clark, C. Silva, R.H. Friend, *J. Chem. Phys.* 130 (2009) 074904.
- [17] K.M. Coakley, B.S. Srinivasan, J.M. Ziebarth, C. Goh, Y. Liu, M.D. McGehee, *Adv. Funct. Mater.* 15 (2005) 1927.
- [18] M. Aryal, K. Trivedi, W. Hu, *ACS Nano* 3 (2009) 3085.
- [19] J.S. Kim, Y. Park, D.Y. Lee, J.H. Lee, J.H. Park, J.K. Kim, K. Cho, *Adv. Funct. Mater.* 20 (2010) 540.